Separation of mitochondria by flow field-flow fractionation for proteomic analysis

Dukjin Kang,[a] Sunok Oh,[a] Pierluigi Reschiglian[b] and Myeong Hee Moon*[a]

Received 31st October 2007, Accepted 3rd January 2008
First published as an Advance Article on the web 22nd February 2008
DOI: 10.1039/b716851a

Flow field-flow fractionation (FlFFF) has been utilized for size-based separation of rat liver mitochondria. Collected fractions of mitochondria of various sizes were examined by confocal microscopy, and mitochondria of each fraction were lysed and analyzed by two-dimensional polyacrylamide gel electrophoresis (2D-PAGE) for the comparison of protein patterns in differently sized mitochondria by densitometric measurements, and for protein characterization of some gel spots with nanoflow liquid chromatography–electrospray ionization-tandem mass spectrometry (nLC–ESI-MS-MS). FlFFF fractions of the mitochondria were also tryptically digested for shotgun proteomic characterization of mitochondrial proteins/peptides by nLC–ESI-MS-MS. Peak area (integrated ion counts) of some peptides extracted from LC–MS chromatograms were examined at different fractions for the quantitative comparison. Among 130 proteins, 105 unique proteins were found to be mitochodrial from the off-line combination of FlFFF and nLC–ESI-MS-MS analysis. It also showed that 23 proteins were found in all fractions but some proteins were found exclusively in certain fractions. Among 25 proteins listed from other subcellular species, seven proteins were known to exist in mitochondria as well as in other subcellular locations, which may support the possible translocation or multiple localizations of proteins among organelles. This study demonstrated effective use of FlFFF for the isolation and/or enrichment of intact mitochondria isolated from cells, as well as its potential use for the fractionation of other subcellular components in the framework of subcellular functional proteomics.

Introduction

The mitochondrion is an essential organelle that plays important roles in energy production, apoptosis, and toxic events of the cell.[1–5] Recent advances in proteomic research have provided more information about mitochondrial proteins for their identification and functions.[2,3,6] In relation to human health, mitochondrial deficiencies or dysfunctions are thought to be related to neurodegenerative diseases such as Parkinson's disease, Alzheimer's disease, Huntington's disease, and even the aging process in general.[1] To study these diseases, a profound understanding of mitochondrial proteins, including their locations, function, and biological pathways, is necessary. In particular, proper isolation and sub-fractionation of mitochondria from cells are important for proteomic analysis since subcellular fractionation increases the probability of identification of low abundance proteins.

Isolation of mitochondria from cells or tissues has been mostly carried out using centrifugation once the cells or tissues are initially disrupted by mechanical or chemical action.[7–9] When differential centrifugation is utilized for isolation of mitochondria, the suspending media, such as Percoll or sucrose, often needs to be removed for further biological assays of extracted mitochondria. Filtration methods using polycarbonate membrane or Nylon filters are used to purify and further sub-fractionate mitochondria from cell extracts following centrifugation.[8,10] However, mitochondria may adhere to the membrane during filtration. In this study, we report a new method for the isolation and fractionation of rat liver mitochondria utilizing flow field-flow fractionation (FlFFF).

FlFFF is one member of the FFF family, which is capable of fractionating particles, cells, proteins or DNA according to size and shape.[11–13] In FlFFF, separation is carried out in an unobstructed channel (*i.e.* without packing material) with an external field (*i.e.* with a crossflow moving across channel) driven to the direction perpendicular to the migration flow (*i.e.* along the channel axis) as shown in Fig. 1. When the crossflow is applied to sample components injected into the FlFFF channel, sample materials are hydrodynamically driven toward one wall (the accumulation wall) of the channel, while simultaneously they diffuse away from the wall due to diffusion. Owing to the balance of the two counter-directed transport mechanisms, sample components find their equilibrium states at a given distance from the wall. The different equilibrium heights reached by the sample components are vertically distributed

[a]*Department of Chemistry, Yonsei University, Seoul, 120-749, South Korea. E-mail: mhmoon@yonsei.ac.kr; Fax: +82 2 364 7050; Tel: +82 2 2123 5634*
[b]*Department of Chemistry "*G. Ciamician*", University of Bologna, Via Selmi 2, I-40126 Bologna, Italy*

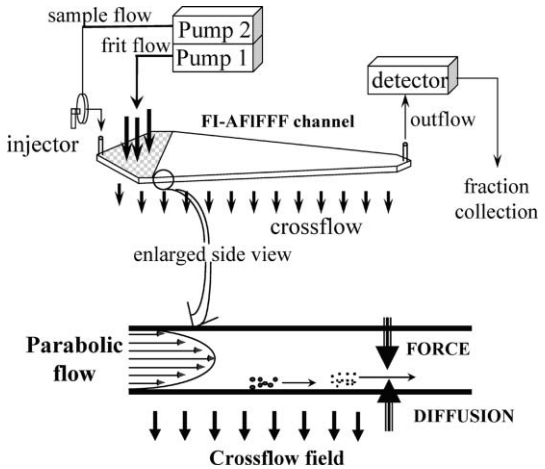

Fig. 1 Schematics of FI-AFlFFF channel with enlarged side view of channel presenting parabolic flow velocity profiles and equilibrium positions of sample components experiencing two opposite forces (crossflow field and diffusion).

from the channel wall, according to differences in the diffusion coefficients (or in the hydrodynamic diameters) of sample species, as shown in Fig. 1. Therefore, the sample components will migrate at different velocities when the axial flow is then applied. Proteins with lower molecular weight (MW) (or smaller hydrodynamic diameter) have larger diffusion coefficient values and they migrate faster at equilibrium positions that are higher than those reached by proteins of higher MW values. Thus, separation in FlFFF is achieved in the order of increasing MW or hydrodynamic diameter of sample components. Since FFF takes place in an open channel, it is generally suited to the gentle separatation of macromolecules and biological particles.

Applications of FFF in biology and biotechnology continue to increase.[14] Sedimentation field-flow fractionation (SdFFF),[12] the FFF subtechnique utilizing centrifugal acceleration as the driving force for sample retention, was first used to fractionate biological particles, such as whole *Escherichia coli* (*E. coli*), that are similar in size and shape to mitochondria from mammalian cells. Gravitational FFF, which utilizes gravity force as an external field, and FlFFF were also utilized to separate deactivated *E. coli*.[15] Hollow-fiber FlFFF (HF FlFFF), the microcolumn variant of FlFFF utilizing a hollow-fiber porous membrane as a channel, separated deactivated *E. coli* and *Vibrio cholerae*.[16,17] Attempts to use SdFFF for micro-preparative isolation of subcellular fractions containing mitochondria, microsomes, Golgi membranes, and plasma membranes of corn roots were also reported.[18] SdFFF, however, requires a highly concentrated sucrose solution to induce the necessary density difference between the organelles and the carrier solution. Since FlFFF retention is not influenced by differences in density between sample components and the carrier solution, it is suitable to separate at high speed less dense biological particles, with the advantage of using biological buffer solutions as mobile phases. It was applied for the separation of bacterial ribosome subunits.[19,20] Recently, few approaches have been made to use FlFFF for proteomics. The on-line hyphenation of HF FlFFF and electrospray ionization-time of flight (ESI-TOF) MS has shown its potential toward the direct characterization of proteome samples at the protein level.[21] Use of microbore HF for microflow HF FlFFF[22] for on-line hyphenation with capillary isoelectric focusing (CIEF) demonstrated that two-dimensional protein fractionation (based on differences in pI and MW) can be achieved in elution mode (*i.e.* in non-gel mode).[23] These studies demonstrated the possibility of utilizing HF FlFFF for protein fractionation at a concentration level that is applicable to protein discovery in proteomics research.

In this study, FlFFF was employed for the first time at a semi-preparative scale for the size separation and simultaneous purification of a mitochondrial extract to carry out multiple secondary analysis for the evaluation of size-dependent mitochondrial protein composition. Compared to earlier FlFFF studies of protein fractionation based on differences in MW, this study guided a potential way to isolate and fractionate organelles such as mitochondria. In this work, a frit-inlet asymmetrical FlFFF (FI-AFlFFF) channel[24] has been employed for the fractionation of mitochondria. FI-AFlFFF is a modified form of FlFFF in which static relaxation of the sample is avoided, which requires a temporary halt of sample migration along the channel. With FI-AFlFFF, the relaxation procedure of mitochondria introduced along with the injection stream is hydrodynamically achieved without stopping the migration flow. During FlFFF separation, size-sorted mitochondria were collected at short time intervals. Mitochondrial fractions of different sizes were examined by confocal microscopy to evaluate size separation and morphology differences. Collected mitochondria were lysed and analyzed by two-dimensional polyacrylamide gel electrophoresis (2D-PAGE) for an initial screening of possible size-based differences in protein content/expression. Some protein spots were excised for in-gel digestion, and the resulting peptides were analyzed by nLC–ESI-MS-MS for protein identification. In addition, each FlFFF fraction of mitochondria was processed for in-solution digestion for shotgun proteomic analysis of proteins.

Experimental

Extraction of rat liver mitochondria

Rat livers were obtained from the Medical Center of Yonsei University. Liver tissues (0.5 g) were suspended with 1 mL of extraction buffer solution (0.1 M phosphate buffer containing 0.05 M sucrose, pH 7.6), and homogenized using a Teflon/Potter homogenizer. Extraction of mitochondria was followed as detailed in the literature.[25] To remove cell debris and nuclei, the homogenized mixture was centrifuged at 600 *g* for 10 min, and the pellet was removed. Then the solution was centrifuged at 11 000 *g* for 15 min to collect the mitochondria-enriched fraction that settled at the tube bottom. The mitochondria-enriched fraction (about 10 μL) was resuspended in 1 mL of buffer solution used as the mobile phase for FlFFF.

Flow FFF operations

A frit-inlet asymmetrical FlFFF (FI-AFlFFF) channel system shown in Fig. 1 was utilized. The FI-AFlFFF channel is a modified form of the FlFFF channel made by introducing a small inlet frit at the inlet end of the depletion wall so that sample relaxation can be hydrodynamically obtained by the compressing action of the frit flow entering through the

small inlet frit.[24,26,27] With a FI-AFlFFF channel, the separation process can be continuous without stopping the flow, thus reducing sample adhesion to the channel wall. Construction of the FI-AFlFFF channel is explained in detail elsewhere.[24,26] The FI-AFlFFF channel spacer was made by cutting a Mylar sheet (170 μm in thickness) with a breadth of 2.0 cm at the inlet side and 1.0 cm at the outlet side. Both ends of the spacer were cut into triangular shapes with lengths of 2.0 and 1.0 cm for the inlet and outlet ends, respectively. Channel tip-to-tip length was 27.2 cm, and the volume was 0.49 mL. At the accumulation channel wall, a PLCGC sheet membrane (MWCO: 10 kDa) from Millipore Corp. (Danvers, MA, USA) was placed above the frit to avoid sample loss through the frit.

The carrier solution used for FlFFF of mitochondria was a 0.1 M phosphate buffered saline (PBS; pH 7.6) solution containing 50 mM sucrose prepared from ultrapure water (>18 MΩ). Prior to use, the solution was filtered through a membrane filter with a pore size of 0.45 μm. The carrier solution and sample suspension were separately delivered by two identical HPLC pumps, Model 930 from Young-Lin Co. (Seoul, Korea). A metering valve, model Whitey SS-22RS2 from the Crawford Fitting Co. (Solon, OH, USA), was located downstream of the detector to provide adequate back-pressure, and to regulate flow rates. Eluted sample components were detected with a Model 730 UV detector (cell volume: 5 μL) from Young-Lin Co. (Seoul, Korea) at a wavelength of 280 nm. For the evaluation of particle separation performance, polystyrene (PS) latex standards (Duke Scientific Co., Palo Alto, CA, USA) with nominal diameter values of 0.222, 0.596, and 1.034 μm were utilized. The carrier solution for PS fractionation contained 0.05% sodium dodecyl sulfate (SDS) and 0.02% NaN_3.

Confocal microscopy of mitochondrial fractions

Mitochondria from each fraction were examined by confocal microscopy using a Model LSM510META from Carl Zeiss (Oberkochen, Baden-Wurttemberg, Germany). Microscopic examination of each mitochondrial fraction collected during the FlFFF runs was performed by the uptake of JC-1 stain, a fluorescent carbocyanine dye (5,5′,6,6′-tetrachloro-1,1′,3,3′-tetraethylbenzimidazolcarbocyanine iodide)[28] purchased from Sigma (St. Louis, MO, USA). Each mitochondrial fraction was resuspended in a 4 mM MOPS [3-(*N*-morpholino)propanesulfonic acid] solution (pH 7.5) containing 20 mM KCl, 2 mM ATP, 2 mM $MgCl_2$, 2 mM sodium succinate, and 0.2 mM EGTA until the final volume of each fraction was 200 μL. Thereafter, 2 μL of JC-1 and 1.8 mL of 4 mM MOPS solution were added to each fraction to make the final volume of 2 mL. For complete uptake of JC-1 dye into the inner membrane of the mitochondria, each fraction was stored for 10 min in a dark room at room temperature. Size calculation of mitochondria at each fraction was obtained by using the Zeiss LSM Image Browser (Ver. 4, 0, 0, 241) from Carl Zeiss.

2D-PAGE of mitochondrial fractions

To extract proteins, each mitochondrial fraction collected from the FlFFF system outlet was lysed in 1.0 mL of a buffer solution consisting of 8 M urea, 2 M thiourea, and 10 mM dithiothreitol (DTT) using tip sonication in an ice bath. Tip sonication was carried out for a total of 50 s (five × 10 s pulses with intervals of 2 s). After lysis, the mixture was filtered with a Microcon YM-3 centrifugal filter unit, and resuspended in a 0.1 M NH_4HCO_3 solution. The protein concentration of each fraction was measured using the Bradford method. A 10 μg sample of protein was suspended in 7 M urea, 2 M thiourea, 0.4% (w/v) DTT, 4% (w/v) 3-[(3-cholamidopropyl)dimethylammonio]-1-propanesulfonate (CHAPS), and 16 μL of protease inhibitor cocktail from Roche Molecular Biochemicals (Indianapolis, IN, USA). Electrophoretic separation of proteins (10 μg) was carried out using a Multiphor II apparatus from GE Healthcare (Bolton, UK) at total 57 kVh on a 7 cm long pH 3–10 IPG strip that was previously hydrated with the same buffer solution. After IEF, PAGE was carried out on 10–18% (v/v) linear-gradient SDS-polyacrylamide gels. After 2D-PAGE, silver staining was made using Vorum's method.[29] The silver-stained gel spots were excised for protein identification by means of nLC–ESI-MS-MS. For the calculation of the spot intensity, a GS-710 Imaging Densitometer from Bio-Rad (Hercules, CA, USA) using ImageMaster 2D software from Amersham Bioscience was utilized.

In-gel enzymatic digestion

Silver-stained protein spots were excised, and in-gel digestion was performed on each spot. Before digestion, the staining reagent was removed by washing the gel band. Gel pieces, each in a 1.5 mL microtube, were destained with 120 μL of a 1 : 1 mixture of 30 mM potassium ferricyanide and 100 mM sodium thiosulfate with vigorous mixing. The destained gel pieces were washed three times with 120 μL of a washing solution containing 50% acetonitrile in 25 mM NH_4HCO_3, pH 7.8, for 10 min. After soaking in acetonitrile for 5 min, gel pieces were vacuum-dried using a Model SC110A Speedvac Plus from the Thermo Electron Corporation (Waltham, MA, USA). For in-gel digestion, dried gel pieces were mixed with 10 μL of a sequencing-grade trypsin solution (0.012 μg μL^{-1} in NH_4HCO_3). After incubation on ice for 45 min, the supernatant was discarded and replaced with 10 μL of 20 mM NH_4HCO_3 at pH = 8.0. Following overnight digestion at 37 °C, 10 μL of 0.5% (v/v) trifluoroacetic acid in 30% CH_3CN was added, and tryptic peptides were extracted by sonication for 40 min in an ultrasonic water bath. The extracted solution was reduced to *ca.* 1 μL by vacuum centrifugation. Peptides were then cleaned up using a Zip-Tip cartridge from Millipore (Billerica, MA, USA), vacuum-dried, and finally resuspended in a solution of 2% CH_3CN and 0.1% formic acid (FA) in water for peptide separation by nLC–ESI-MS-MS.

In-solution enzymatic digestion

Mitochondria in each FlFFF fraction were lysed by tip sonication. After the Bradford test, each fraction was dried and resuspended at a concentration of 100 μg μL^{-1} in a solution of 8 M urea, 0.1 M NH_4HCO_3, and 10 mM dithiothreitol for 2 h at 37 °C. For alkylation of the thiol groups the mixture was treated with iodoacetamide at a total concentration of 20 mM for 2 h at 0 °C in the dark. An excess of cysteine (40×) was added to remove excess iodoacetamide, and then the mixture

was diluted to a 1.0 M urea concentration. Proteomics-grade trypsin (Sigma, St. Louis, MO, USA) was added at a ratio of 1 : 50 (trypsin : protein), and the mixture was incubated for 24 h at 37 °C. After digestion, tosyl-L-lysyl-chloromethane ketone hydrochloride (TLCK) was added to stop digestion at a 10 : 1 molar ratio of TLCK : trypsin. Finally, the digested mixture was desalted using an Oasis HLB cartridge (Waters, Millford, MA, USA), then dried and resuspended in 2% CH_3CN + 0.1% FA in water before nLC–ESI-MS-MS analysis.

nLC–ESI-MS-MS of mitochondrial digests

A home-made, reversed-phase, capillary LC column (170 mm × 75 μm) packed with 3 μm 100 Å Magic C18AQ from Michrom BioResources Inc. (Auburn, CA, USA) was used. The detailed procedure to prepare the capillary LC column is described in the literature.[23,30,31] The column with a pulled tip was interfaced without a separate emitter to the electrospray ionization (ESI) source of an ion-trap mass spectrometer LCQ Deca Max (Thermo Finnigan, San Jose, CA, USA). A precolumn was used to desalt and remove impurities in the peptide samples. The precolumn was made using a silica tube (200 μm id, 360 μm od) with an end frit (2 mm in length) prepared by a sol–gel method.[31] It was packed with 5 μm 200 Å Magic C18AQ for 1.0 cm. The precolumn was connected to the capillary column through a PEEK microcross from Upchurch Scientific, Inc. (Oak Harbor, WA, USA). A platinum wire was connected to the microcross to supply the ESI voltage. Detailed configuration of this coupling is described elsewhere.[30,31]

A Model 2200 capillary flow HPLC system from Agilent Technologies (Palo Alto, CA, USA) was used. A 2.0 μL (about 4 μg for each fraction) aliquot of the sample was injected by an autosampler into the precolumn. Binary-gradient separations were performed at a 200 nL min^{-1} flow rate. Mobile-phase components were: (A) 2% CH_3CN in water, and (B) 95% CH_3CN in water; both were added with 0.1% FA. For analysis of the digests from the 2D-PAGE spots, the gradient began with (I) 5% B for 5 min. Then the percentage of B was increased according to the following steps: (II) 12% in 5 min, (III) 18% in 20 min, (IV) 30% in 30 min, and (V) 80% in 3 min. Step (V) was held for 10 min to clean the column. Step B was then decreased to 5% in 2 min, and it remained at that concentration for at least 25 min for column reconditioning before the next run. For the analysis of digests directly obtained from FlFFF fractions, the gradient program was similar to the program described above, with the exception that the level of step (II) was reached in 15 min, that of step (III) in 25 min, and that of step (IV) in 90 min.

The nLC eluate was electrosprayed directly into the mass spectrometer. A voltage of 2.0 kV in positive ion mode was applied through the Pt wire connected to the microcross. MS analysis was carried out by a precursor scan (300–1800 amu) followed by three data-dependent MS-MS scans. MS-MS spectra were analyzed using the Sequest program with rat proteome database from NCBI. Results were confirmed also using the database from Swissprot. Both databases were upgraded to the most recent versions before use. The mass tolerance between the measured monoisotopic mass and the calculated mass was 1.0 u for the molar mass of a precursor peptide and 1.0 u for the mass of peptide fragment ions. For data screening, only peptides yielding minimum delta-correlation (ΔCn) scores of 0.1 and cross-correlation (Xcorr) values larger than 2.0, 2.5, and 3.3 for singly-, doubly-, and triply-charged ions, respectively, were selected for extensive homology. For the comparison of relative abundances of peptides among different FlFFF fractions, chromatograms of a same peptide from different FlFFF fractions were extracted from the precursor run, and the peak areas were calculated using BioworksBrowser software (Ver. 3.2 EF 2) from Thermo Finnigan.

Results and discussion

Fig. 2 shows the fractogram of the separated mitochondria (upper plot) and the superimposed fractogram of polystyrene (PS) latex mixtures (lower plot). Both fractograms were obtained under the same run conditions: sample flow/frit flow rate = 0.15/5.0 mL min^{-1}, outflow/crossflow rate = 0.30/4.85 mL min^{-1} (each flow is marked in Fig. 1). The PS fractogram demonstrates that, according to the normal mode, nanosized particle retention increased with increasing particle size. This is because a small particle, having a larger diffusion, overcomes the field force and it is swept further down the channel from the accumulation wall than a large particle. For mitochondria, the same run conditions for the PS separation were selected and the fractogram is reported in the upper plot of Fig. 2. As observed from PS separation it was expected that separation of mitochondria was achieved with an increasing order of diameter. At the beginning of elution, a sharp peak appeared (within the fraction 1), which was presumably a void peak, followed by two main peaks. This was confirmed by further microscopic examination. The injected amount of sample was 10 μL of the resuspended mitochondria sample (1 mL in final volume) from the extraction procedure described in the Experimental section. The injected amount was equivalent to 1/100 of the total amount of the mitochondrial fraction extracted from 0.5 g of rat liver tissue.

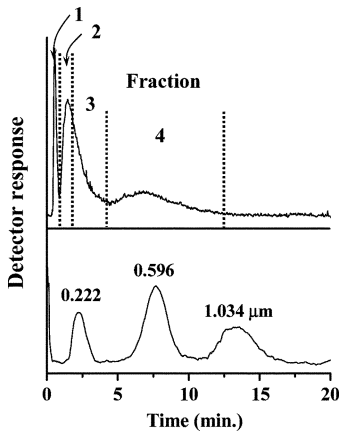

Fig. 2 Fractogram of mitochondrial extracts from rat liver by FI-AFlFFF compared with separation of PS standard latex particles. Injection flow/frit flow rate = 0.15/5.0 mL min^{-1}, outflow/crossflow rate = 0.30/4.85 mL min^{-1}. Mobile phase: 0.1 M sodium phosphate (without sucrose) for mitochondria. Fractionated mitochondria (fractions 1–4) were collected at time intervals of 0–1.1, 1.1–2.1, 2.1–4.1, and 4.1–12.6 min, respectively. Elution time from the UV detector outlet tubing was 6 s.

Eluting mitochondria were collected at time intervals as marked in Fig. 2. Collected mitochondria at each fraction were examined using a confocal microscope. Fig. 3 presents the confocal micrographs of the collected particles of the four fractions. It shows that very small mitochondria (along with some aggregates) eluted in fraction 1, and that their sizes appear to be similar to those found in fraction 2. This could be explained by co-elution of some mitochondria that were not fully relaxed during hydrodynamic relaxation. This is a drawback of utilizing hydrodynamic relaxation compared to what can be obtained from the static stop-flow relaxation procedure. Nonetheless, hydrodynamic relaxation reduces the risk of sample adhesion at the channel wall due to the elimination of stop-flow relaxation. However, micrographs of later fractions showed that mitochondrial size increased with increasing fraction number (fractions 3 and 4).

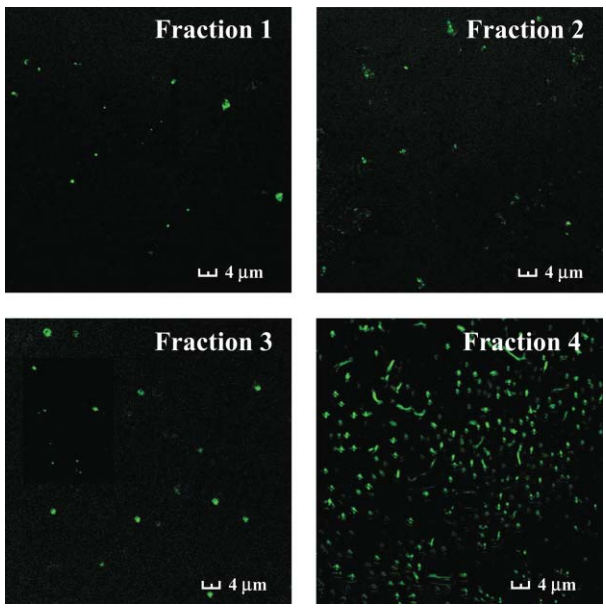

Fig. 3 Confocal microscopic images of each fraction collected during the FFF run. To assess the morphology and genuineness of the mitochondria in each fraction, JC-1 stain was used to verify the mitochondrial inner membrane integrity. All images were obtained by observing the emission wavelength of 590 nm.

While the mitochondria in earlier fractions were rather spherical, fraction 4 appeared to contain both spherical and elongated mitochondria. The average diameter of the mitochondria in each fraction was obtained by image analysis. The results of size measurements for each fraction are listed in Table 1. As the fraction number increased, the average length increased from 0.54 ± 0.20 μm for fraction 1 to 1.11 ± 0.47 μm for fraction 4. Mitochondria of about 1 μm in length eluted at a retention time approximately 37% shorter than was expected from the retention of PS particles of similar sizes. This was likely due to shape effects which led to an elevation of the equilibrium position of the non-spherical particles, leading to a shorter retention time.[32] There is a possibility of shape deformation of the mitochondria during hydrodynamic relaxation, since a relatively high speed frit flow (which was 33 times faster than the sample flow in this experiment) that enters from the inlet frit pushes incoming mitochondria toward the channel wall. However, it is difficult to assess the contribution of shape deformation in this study since mitochondria morphology varies from tubular to oval shape.

Table 1 Average diameter of the mitochondria of each fraction obtained from image analysis

Fraction no.	Time/min	Av. diameter/μm	Counted numbers
1	0.00–1.10	0.54 ± 0.20	22
2	1.10–2.10	0.56 ± 0.19	27
3	2.10–4.10	0.86 ± 0.27	32
4	4.10–12.6	1.11 ± 0.47	47

Mitochondria collected at each fraction were lysed to study protein patterns. Resulting proteins were analyzed in part with 2D-PAGE, and the rest were further digested for shotgun analysis using nLC–ESI-MS-MS. Each 10 μg of protein extract was loaded into a 2D-polyacrylamide gel. Gel images of mitochondrial proteins of each fraction are shown in Fig. 4. Gel images of fractions 1 and 2 appear to be similar to each other in the distribution of protein spots. Fractions 3 and 4 had similar distributions and intensities of protein spots, but they were significantly different from the gel image of fraction 2. To identify proteins of gel spots showing different intensities, some spots (marked as 1–6 in the gel image of fraction 2 in Fig. 4) were excised, then followed by in-gel digestion with trypsin for nLC–ESI-MS-MS analysis of peptides. The MS-MS spectrum of a peptide from gel spot 4 is shown in Fig. 5. A database search against NCBI resulted in a peptide ion, R.FDAGELITQR.E (m/z 575.6, $[M + 2H^+]^{2+}$) from prohibitin, which is known to inhibit DNA synthesis and to play a role in regulating mitochondrial respiration activity. Proteins found from the gel spots are listed in Table 2 along with the

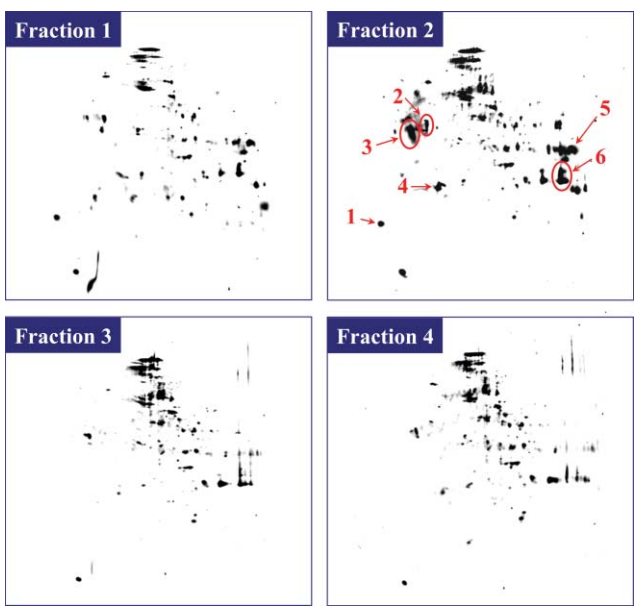

Fig. 4 SDS-PAGE gel image of mitochondrial proteins of each FlFFF fraction showing heterogeneous protein species according to their retention times. Each gel was loaded with 10 μg of mitochondrial lysate of each fraction.

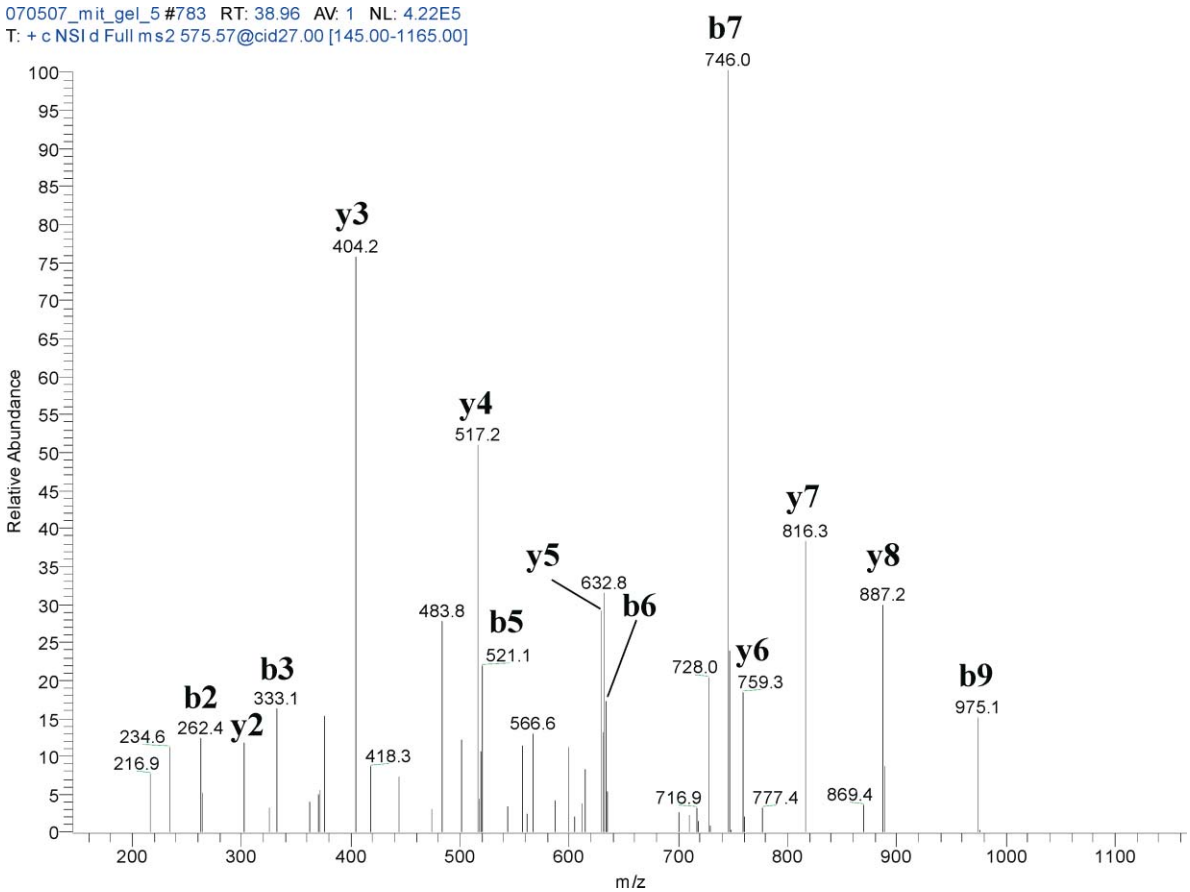

Fig. 5 CID spectrum of ion m/z 575.6 $(M + 2H^+)^{2+}$ of R.FDAGELITQR.E from prohibitin performed by nLC–ESI-MS-MS after in-gel digestion of spot number 4 of fraction 2.

Table 2 Proteins found from the gel spots of the 2D-PAGE image by nLC–ESI-MS-MS and the relative percentage of spot intensity at each fraction by image densitometer

			Percentage of spot (relative ratio)			
			Fraction number of FFF			
Spot	gi_number	Protein	1	2	3	4
1	gi_11120720	Membrane-associated progesterone-receptor component 1	1.90 (1.00)	0.94 (0.49)	0.11 (0.05)	0.11 (0.05)
2	gi_51948476	Ubiquinol-cytochrome c reductase core protein I, beta subunit	1.76 (1.00)	3.90 (2.21)	0.58 (0.33)	0.58 (0.32)
3	gi_54792127	ATP synthase, H+ transporting, mitochondrial F1 complex	2.32 (1.00)	6.23 (2.68)	5.03 (2.16)	4.87 (2.10)
4	gi_62664759	Prohibitin	4.04 (1.00)	2.42 (0.60)	1.25 (0.31)	1.25 (0.31)
5	gi_18426866	Acetyl-coenzyme A acyltransferase 2	3.52 (1.00)	4.64 (1.32)	0.60 (0.17)	0.57 (0.16)
6	gi_20127395	Urate oxidase	8.32 (1.00)	8.05 (0.97)	2.48 (0.30)	2.45 (0.29)

relative percentage of spot intensity at each fraction obtained by densitometric analysis. These proteins were found to be located in the mitochondria except for spot 1, according to the NCBI database. However, the spot 1 protein was reported in the literature to be a mitochondrial protein, as will be discussed later. Gel spot 1 in fraction 2 was found to be the membrane-associated progesterone-receptor component 1, which functions as an electron carrier for membrane-bound oxygenase. This protein spot also appeared in the gel image of fraction 1, but it did not appear in the gel images of fractions 3 and 4. This protein was found to be from the endoreticulum (ER) in the NCBI database, but it was also reported to be found in

Table 3 Comparison of peak area from extracted chromatograms of peptides found at different FlFFF fractions by shotgun nLC–ESI-MS-MS. Corresponding proteins of peptides were the same as found from spot numbers 5 and 6 listed in Table 2

	Peak area ($\times 10^9$), ($n = 3$)			
	Fraction number of FI-AFlFFF			
Protein/peptides from shotgun nLC–ESI-MS-MS	1	2	3	4
Acetyl-coenzyme A acyltransferase 2 (same as found in spot 5)				
R.AALSAGKVPPETIDSVIVGNVMQSSSDAAYLAR.H	2.1 ± 0.0 (1.00)	1.7 ± 0.1 (0.81)	0.5 ± 0.3 (0.24)	0.5 ± 0.1 (0.24)
K.SLDLDPSKTNVSGGAIALGHPLGGSGSR.I	4.5 ± 0.3 (1.00)	3.4 ± 0.5 (0.76)	0.7 ± 0.4 (0.16)	0.9 ± 0.6 (0.20)
R.WKAANEAGYFNEEMAPIEVK.T	0.9 ± 0.1 (1.00)	1.8 ± 0.3 (2.0)	0.4 ± 0.2 (0.44)	0.5 ± 0.2 (0.56)
Urate oxidase (same as found in spot 6)				
K.MGLINKEEVLLPLDNPYGK.I	1.6 ± 0.7 (1.00)	4.7 ± 0.2 (2.93)	0.6 ± 0.4 (0.38)	0.8 ± 0.3 (0.50)
K.TTQSGFEGFIKDQFTTLPEVKDR.C	3.2 ± 0.5 (1.00)	6.3 ± 0.9 (1.97)	0.2 ± 0.1 (0.06)	0.5 ± 0.1 (0.16)

mitochondria, as will be discussed later. However, the relative spot intensities of spot 1 in fractions 3 and 4 were 0.11%, which was a decrease to *ca.* 5% when compared to the intensity in fraction 1, as listed in Table 2. For 2D-PAGE analysis of each fraction, the same amount of protein was loaded. Gel spots 2 and 3 appeared to be intense in fraction 2, but the relative intensity measured at fraction 2 increased, and decreased for the larger fraction numbers. However, similarly to spot 1, spot 4 appeared in all fractions in Fig. 3, and the intensity among the fractions decreased gradually, to 60% at fraction 2 and to 31% for both fractions 3 and 4 as mitochondrial size increased. Spots 5 and 6 were well evident in both fractions 1 and 2, but spot 5 was relatively weak in intensity in fractions 3 and 4. Though the intensities of proteins found from spots 2–6 were different in each fraction, these five proteins were found in all fractions when the digests of each fraction were analyzed by shotgun nLC–ESI-MS-MS. Differences in spot intensities among the fractions may suggest that different protein abundances in the extracts are from mitochondria of various sizes.

Additional indications of differences in protein composition of the mitochondrial fractions were examined by direct shotgun analysis. Each fraction was lysed and digested in solution, and the resulting peptide mixtures were run three times by nLC–ESI-MS-MS. The peak areas (integrated ion counts over the peptide elution time from the nLC–MS chromatogram) of some peptides were compared at different FlFFF fractions, according to the method reported in the literature.[33,34] Among the six proteins found in 2D-PAGE followed by nLC–ESI-MS-MS, two proteins (found from spots 5 and 6) were found from shotgun analysis with exactly the same peptides, respectively, and the peak areas of the extracted chromatogram from direct LC–ESI-MS of each fraction digests were semi-quantitatively compared. For instance, comparisons were made with three common peptides from acetyl-coenzyme A acyltransferase 2 from shotgun analysis. For this protein, more than ten different peptides were found, but only three peptides were found in all FlFFF fractions, and the peak areas were compared as listed in Table 3. Among the peptides matched from database, R.AALSAGKVPPETIDSVIVGNVMQSSSDAAYLAR.H (m/z 1107.3, $[M + 3H^+]^{3+}$, $t_r = 79.2 \pm 1.3$ min for all four fractions) was observed in all four fractions by direct nLC–ESI-MS-MS of each of the fraction digests. The relative deviation of retention time values among different fractions was 1.7% ($n = 3$). When the peak areas of the extracted chromatograms from all fractions were compared, it showed a gradual decrease as the fraction number increased (Table 3). The relative change was to 24% for fractions 3 and 4 (compared with the relative percentage of area of fraction 1), and this trend was similar to the 2D-PAGE result of spot 5 in Table 2. Each peak area was reported as an average value from three different runs of nLC–ESI-MS-MS. Another peptide from the same protein listed in Table 3, K.SLDLDPSKTNVSGGAIALGHPLGGSGSR.I (m/z 888.8, $[M + 3H^+]^{3+}$, $t_r = 49.4 \pm 1.8$ min), showed a similar trend as the peptide above mentioned. The third peptide, R.WKAANEAGYFNEEMAPIEVK.T (m/z 843.3, $[M + 3H^+]^{3+}$, $t_r = 55.2 \pm 1.9$ min) showed a slightly different pattern in which the relative peak area increased in fraction 2 but then dropped down to 44% for fraction 3. A similar trend of peak area decrease was found with two peptides from urate oxidase, which were also found in spot 6 in Table 2. The peak area of peptide K.MGLINKEEVLLPLDNPYGK.I (m/z 924.3, $[M + 3H^+]^{3+}$, $t_r = 65.0 \pm 1.7$ min) from urate oxidase increased for fraction 2 but then decreased to 38 and 50% in fractions 3 and 4 as listed in Table 3, respectively. While the 2D-PAGE peak intensity did not show an increase for fraction 2 (see Table 2), it showed a decrease in fractions 3 and 4 to about 30% compared with the intensity of fraction 1. Though the comparison based on peak area measurements was not as accurate as could be expected from using isotope or chemical labeling methods, the peak area comparisons in conjunction with 2D-PAGE spot intensity measurements showed an estimate of the relative protein abundance. In addition, this study showed that when dealing with particular organelles in cells, fractions collected from FlFFF runs can be utilized for secondary analysis techniques.

Mitochondrial proteins from each fraction found by shotgun analysis are listed in Table 4 according to their location.

Table 4 Proteins with their subcellular locations obtained by nLC–ESI-MS-MS specified with the corresponding FlFFF fractions

gi_number: found proteins	Subcellular location	Fraction number			
		1	2	3	4
gi|1154950: choline dehydrogenase; gi|13937353: prohibitin; gi|13994225: hydroxysteroid (17-beta) dehydrogenase 10; gi|17978459: ATP synthase, H+ transporting, mitochondrial F0, subunit E; gi|18426858: succinate dehydrogenase complex, subunit A, flavoprotein; gi|18426866: acetyl-coenzyme A acyltransferase 2; gi|20127395: urate oxidase; gi|20302061: mitochondrial ATP synthase, O subunit; gi|24233541: cytochrome c oxidase, subunit Va; gi|25742739: acyl-CoA synthetase long-chain family member 1; gi|34879019: protein NipSnap1; gi|40538742: ATP synthase, H+ transporting, mitochondrial F1, alpha subunit, isoform 1; gi|51948476: ubiquinol-cytochrome c reductase core protein I; gi|54792127: ATP synthase, H+ transporting, mitochondrial F1, beta subunit; gi|55741544: ubiquinol-cytochrome c reductase core protein II; gi|55742813: 3-hydroxybutyrate dehydrogenase; gi|55971: cytochrome c oxidase subunit Va preprotein; gi|55992: cytochrome c oxidase subunit Via; gi|57114330: ubiquinol-cytochrome c reductase, Rieske iron-sulfur polypeptide 1; gi|61556754: B-cell receptor-associated protein 37; gi|6729934: chain A, rat liver F1-ATPase; gi|6981420: pancreatic trypsin 1; gi|8393186: carbamoyl-phosphate synthetase 1, mitochondrial	Mitochondria	○	○	○	○
gi|109468302: NADH dehydrogenase (ubiquinone) 1 alpha subcomplex 7; gi|202727: alcohol dehydrogenase; gi|6981010: hemoglobin alpha 1 chain	Mitochondria	○	○	○	
gi|47058994: ATP synthase, H+ transporting, mitochondrial F0, subunit G; gi|60551387: arginase 1; gi|13786200: voltage-dependent anion channel 1	Mitochondria	○	○		○
gi|109465447: similar to cytochrome c oxidase, subunit VIb polypeptide 1; gi|56188: glyceraldehyde 3-phosphate-dehydrogenase; gi|728931: ATP synthase gamma chain, mitochondrial; gi|929988: pyruvate carboxylase	Mitochondria		○	○	○
gi|52138635: electron-transferring-flavoprotein dehydrogenase; gi|77736544: cytochrome c oxidase, subunit VIa, polypeptide 1; gi|82617686: NADH dehydrogenase (ubiquinone) 1 beta subcomplex, 4, 15 kDa; gi|19424338: mitochondrial trifunctional protein, beta subunit	Mitochondria	○	○		
gi|13540663: betaine-homocysteine methyltransferase; gi|1619606: aldolase B; gi|19173788: solute carrier family 25, member 10; gi|19424318: enoyl-coenzyme A, hydratase/3-hydroxyacyl-coenzyme A dehydrogenase; gi|2494234: trifunctional enzyme alpha subunit, mitochondrial precursor; gi|31543464: pyruvate carboxylase; gi|32482836: low molecular mass ubiquinone-binding protein; gi|483109: hemoglobin alpha-2 chain; gi|61557127: nicotinamide nucleotide transhydrogenase; gi|62646841: calcium-binding mitochondrial carrier protein Aralar2; gi|62652158: similar to 13 kDa differentiation-associated protein; gi|8393913: propionyl-coenzyme A carboxylase, beta polypeptide	Mitochondria				
gi|27663138: similar to NADH dehydrogenase 1 alpha subcomplex, 6	Mitochondria	○		○	
gi|109509350: similar to glutathione *S*-transferase, theta 3	Mitochondria				
gi|8393180: cytochrome c oxidase subunit IV isoform 1	Mitochondria	○			○
gi|109510368: similar to NADH-ubiquinone oxidoreductase MWFE subunit; gi|139948224: succinate-CoA ligase, GDP-forming, alpha subunit; gi|27717677: similar to NADH oxidoreductase	Mitochondria		○	○	
gi|9506411: ATP synthase, H+ transporting, mitochondrial F0, subunit d	Mitochondria		○		○
gi|16758362: cytochrome c oxidase subunit Vb; gi|20806141: solute carrier family 25, member 3; gi|77157805: methionine adenosyltransferase I, alpha	Mitochondria			○	○
gi|109465447: cytochrome c oxidase, subunit VIb polypeptide 1; gi|145651820: aldehyde dehydrogenase family 6, subfamily A; gi|16758586: succinate-CoA ligase, GDP-forming, alpha subunit; gi|17985949: hemoglobin beta chain complex; gi|19705543: MOCO sulfurase C-terminal domain containing 2; gi|20302049: diaphorase 1; gi|203921: D-beta-hydroxybutyrate dehydrogenase; gi|21245098: tubulin, beta 3; gi|2961553: amyloid beta-peptide-binding protein; gi|296485: chaperonin 10; gi|395943: III beta-3 globin	Mitochondria				
gi|452977: fatty acid-binding protein FABP-1; gi|51092268: NADH dehydrogenase (ubiquinone) flavoprotein 2; gi|62647466: inner membrane protein, mitochondrial; gi|62649444: cytochrome P450, family 4, subfamily a, polypeptide 14; gi|6980956: glutamate dehydrogenase 1; gi|6981050: hydroxy-delta-5-steroid dehydrogenase; gi|6981450: ATP-binding cassette, sub-family D (ALD), member 3; gi|9506509: cytochrome c oxidase, subunit VIc	Mitochondria	○			

Table 4 (*Contd.*)

gi_number: found proteins	Subcellular location	Fraction number 1	2	3	4
gi|109478298: similar to voltage-dependent anion-selective channel protein 1; gi|109498024: similar to SMG-7 homolog; gi|19705465: ATP synthase, H+ transporting, mitochondrial F0, subunit b, isoform 1; gi|25453414: arginosuccinate synthetase; gi|27682913: similar to NADH dehydrogenase 1 alpha subcomplex, 2 gi|395937: beta-2 globin; gi|56553829: chain C, arginase-F2-L-arginine complex; gi|58865926: methylcrotonoyl-coenzyme A carboxylase 2; gi|62641274: similar to Tu translation elongation factor, mitochondrial; gi|6980972: glutamate oxaloacetate transaminase 2	Mitochondria		○		
gi|109468417: similar to mitochondrial carrier homolog 2; gi|19705453: microsomal glutathione *S*-transferase 1; gi|27671040: similar to ATP synthase D chain, mitochondrial; gi|27702072: similar to NADH dehydrogenase Fe–S protein 3; gi|32189350: solute carrier family 25, member 5; gi|39930503: ATP synthase, H+ transporting, mitochondrial F1, gamma subunit; gi|51260066: propionyl-coenzyme A carboxylase, beta polypeptide; gi|56383: heat shock protein (hsp60) precursor; gi|56789874: hydroxysteroid (17-beta) dehydrogenase 9; gi|56961620: heterogeneous nuclear ribonucleoprotein M; gi|57029: H(+)-transporting ATP synthase; gi|62642368: similar to NADH dehydrogenase (ubiquinone) 1 beta subcomplex 8	Mitochondria			○	
gi|21617859: serine dehydratase; gi|27465521: 3-hydroxy-3-methylglutaryl-coenzyme A synthase 2; gi|53850628: NADH dehydrogenase (ubiquinone) Fe–S protein 1, 75 kDa; gi|6978725: cytochrome c, somatic; gi|76096306: vesicle amine transport protein 1 homolog	Mitochondria				○
gi|223556: **tubulin alpha**	Nucleus	○		○	○
gi|57353: TH2B histone; gi|27465535: **tubulin, beta 5**; gi|40018568: **tubulin, beta, 2**	Nucleus				
gi|62652148: similar to transcription factor Spi-C; gi|62663604: similar to histone H2B 291B	Nucleus	○			
gi|62650831: similar to small nuclear RNA activating complex, polypeptide 1	Nucleus			○	
gi|6981486: ribophorin I	ER	○		○	○
gi|2257955: **cytochrome b5**	ER			○	○
gi|21426797: flavin containing monooxygenase 5; gi|11120720: **progesterone-receptor membrane component 1**	ER	○			
gi|58585242: retinol dehydrogenase 7	ER			○	
gi|549157: **UDP-glucuronosyltransferase 2B12 precursor**	ER				○
gi|55765: aryl sulfotransferase	Cytoplasm	○			○
gi|27695749: **similar to glyceraldehyde-3-phosphate dehydrogenase**; gi|6978681: catechol-*O*-methyltransferase	Cytoplasm				○
gi|109487877: similar to golgi autoantigen, golgin subfamily a, 4	Golgi	○			
gi|8393215: CTL target antigen	Unknown	○	○	○	
gi|109480482: similar to 13 kDa differentiation-associated protein	Unknown				
gi|109510879: similar to oligophrenin 1; gi|110347600: tubulin, beta-like; gi|7513957: cytochrome-c oxidase chain VIIa	Unknown		○		
gi|285058: macrophage migration inhibitory factor homolog	Unknown			○	
gi|109483662: similar to guanine nucleotide exchange factor p532	Unknown				
gi|3885972: 270 kDa ankyrin G isoform	Unknown				○

Proteins of unknown location are also reported. Among the total of 130 proteins found from all fractions, 105 were listed as mitochondrial proteins in the NCBI database. Among the 105 mitochondrial proteins found in this experiment, 68 proteins were found exclusively in fraction 1, which contained the smallest mitochondria. Only 23 proteins were found in all fractions. Among these proteins, five of them were found in five of the 2D-PAGE spots 2–6. While the protein acetyl-coenzyme A acyltransferase 2, found at gel spot 5 in Fig. 4, showed weak intensities at fractions 3 and 4, it was also found in all the fractions using direct nLC–ESI-MS-MS. Six other proteins were found in three of the fractions (fractions 1–3 or 1, 2, and 4). Thirteen proteins that were not found in fraction 2 were found in fractions 1 and 3, while four other proteins were, conversely, found in all fractions except fraction 1. These findings suggest that there was a difference in protein composition along the fractions of differently sized mitochondria.

In Table 5, all proteins found in the four fractions are classified by their locations within the cell. Though the extraction procedure to isolate mitochondria from cells was carefully applied, 25 proteins from subcellular locations other than mitochondria were found in all of the fractions. For instance, a total of seven nucleus proteins was found, but six of them were from fraction 1. The possibility of the co-existence of the nucleus

Table 5 Number of found proteins in each FlFFF fraction of mitochondrial extracts counted by subcellular locations

	No. of proteins (multiple peptide identification)			
	Fraction 1	Fraction 2	Fraction3	Fraction 4
Mitochondrial	62 (55)	51 (40)	61 (53)	41 (31)
From other locations	12 (7)	5 (5)	7 (3)	9 (3)
Unique proteins	79	22	19	10
Total number of unique proteins	130			

in the fractions is relatively low since few nucleus proteins were found from fraction 1. It is possible that some of the nucleus proteins found were translocating within subcellular species. It is known that proteins can be exchanged among different subcellular units and, therefore, they can be found in the proteome of subcellular units where, based on current knowledge, they are not expected to be. For instance, the three tubulin proteins (alpha, beta 2, and beta 5 in bold type in Table 4), which were classified as nucleus proteins by the protein database, were reported to be found at the mitochondrial membrane and other subcellular organelles.[35,36] Among six endoreticulum (ER) proteins listed in Table 4, cytochrome b5 was reported to exist at both the ER and the mitochondrial outer membrane,[37,38] and the progesterone-receptor membrane component 1 and UDP-glucuronosyltransferase 2B12 precursor were found to exist at the ER, cell surface, microsol and mitochondrial integral membrane as well.[37,39,40] In addition, a cytoplasmic protein (a protein similar to glyceraldehyde-3-phosphate dehydrogenase) was reported as a mitochondrial protein.[36] In our survey, seven among 25 proteins listed as non-mitochondrial proteins were found to exist in mitochondria and other subcellular locations. There is a possibility that the remaining 18 proteins can be candidates to be translocating proteins. This presents a challenge to the combined analytical methods used in this study that can be applied for subcellular proteomics. Altogether, among the 130 proteins found from the four fractions, 105 unique mitochondrial proteins were classified by their cellular functions in Table 5. Among them, 60 proteins are classified as carriers/transporters and another 32 proteins are involved in metabolism, as listed in Table 6.

Table 6 Characteristic functions of mitochondrial proteins by nLC–ESI-MS-MS

Functional categories	No. of mitochondrial proteins found
Carriers/transporters	60
Nucleic acid metabolism	11
Oxidative phosphorylation	1
Amino acid metabolism	8
Fatty acid metabolism	7
Stress response	2
Nitrogen metabolism	1
Protein sorting	3
Carbohydrate metabolism	5
Unknown	7

Conclusions

In this study, FlFFF was demonstrated to effectively fractionate rat liver mitochondria according to size differences. Fractionated mitochondria were collected for the identification of proteins. From a comparison between the results obtained by off-line coupling of 2D-PAGE with nLC–ESI-MS-MS and the results from shotgun analysis of the digests of fractionated mitochondrial extracts using nLC–ESI-MS-MS, it is suggested that the protein composition of mitochondria may vary upon size. A quantitative evaluation of possible differences in protein expression as a function of mitochondrial size was not performed. To that end, the use of quantitative methods in MS-based proteomics using protein tagging would be particularly useful. However, since different proteins were found in fractions of differently sized mitochondria, we concluded that FlFFF may be potentially useful for subcellular, functional proteomics. This possibility should be further investigated when a more systematic experimental design for properly evaluation of the effective ability of FlFFF to isolate mitochondria completely from other organelles is developed.

Results of the current study are not compared to what could be obtained using the density-gradient sedimentation technique, which is a well-established though rather time-consuming method for the preparative separation of organelles. This is because FlFFF provides a high-speed size-based separation which is independent of the density of the sample components. FlFFF can then be utilized either with or without coupling with density-gradient sedimentation. In the case of FlFFF in combination of density-gradient fractionation, we expect that it should enhance the resolution of subcellular components of the same density but of different size. If used as a stand-alone method, FlFFF may provide size separation of organelles reducing the risk of co-elution with free proteins. However, should a direct comparison of the two methods be done, it must be noted that cell homogenates (*i.e.* without complete lysis) should be considered as the starting samples. This approach may be an interesting object of future studies.

Acknowledgements

This work was supported by grant No. R01-2006-000-10004-0 from the Basic Research Program of the Korea Science & Engineering Foundation and partly by the Korea Foundation for International Cooperation of Science & Technology (KICOS) through a grant provided by the Korean Ministry of Science & Technology (MOST) in K20713000009-07b0100-00910.

References

1 I. E. Scheffler, *Mitochondron*, 2001, **1**, 3–31.
2 M. Fountoulakis, P. Berndt, H. Langen and L. Suter, *Electrophoresis*, 2002, **23**, 311–328.
3 D. Pflieger, J.-P. Le Caer, C. Lemaire, B. A. Bernard, G. Dujardin and J. Rossier, *Anal. Chem.*, 2002, **74**, 2400–2406.
4 B. Conradt, *Nature*, 2006, **443**, 646–647.
5 H. M. McBride, M. Neuspiel and S. Wasiak, *Curr. Biol.*, 2006, **16**, R551–R560.
6 V. Anesti and L. Scorrano, *Biochim. Biophys. Acta*, 2006, **1757**, 692–699.
7 C. V. Lusena, *Can. J. Biochem.*, 1968, **46**, 879–883.
8 C. Bai, C. W. Slife, T. Y. Aw and D. P. Jones, *Anal. Biochem.*, 1989, **179**, 114–119.
9 J. R. Yate, 3rd, A. Gilchrist, K. E. Howel and J. M. Bergeron, *Nature*, 2005, **6**, 702–714.
10 T. Hajek, D. Honys and V. Capkova, *Plant Sci.*, 2004, **167**, 389–395.
11 J. C. Giddings, F. J. Yang and M. N. Myers, *Science*, 1976, **193**, 1244–1245.
12 J. C. Giddings, *Science*, 1993, **260**, 1456–1465.
13 M. E. Schimpf, K. D. Caldwell and J. C. Giddings, *Field-Flow Fractionation Handbook*, Wiley Interscience, New York, 2000.
14 P. Reschiglian, A. Zattoni, B. Roda, E. Michelini and A. Roda, *Trends Biotechnol.*, 2005, **23**, 475–483.
15 P. Reschiglian, A. Zattoni, B. Roda, S. Casolari, M. H. Moon, J. Lee, J. Jung, K. Rodmalm and G. Cenacchi, *Anal. Chem.*, 2002, **74**, 4895–4904.
16 P. Reschiglian, B. Roda, A. Zattoni, B. Min and M. H. Moon, *J. Sep. Sci.*, 2002, **25**, 490–498.
17 P. Reschiglian, A. Zattoni, B. Roda, L. Cinque, D. Melucci, B. R. Min and M. H. Moon, *J. Chromatogr., A*, 2003, **985**, 519–529.
18 S. M. Mozersky, K. D. Caldwell, S. B. Jones, B. E. Maleeff and R. A. Barford, *Anal. Biochem.*, 1988, **172**, 113–123.
19 M. Nilsson, S. Birnbaum and K.-G. Wahlund, *J. Biochem. Biophys. Methods*, 1996, **33**, 9–23.
20 M. Nilsson, K.-G. Wahlund and L. Bulow, *Biotechnol. Tech.*, 1998, **12**, 477–480.
21 P. Reschiglian, A. Zattoni, B. Roda, L. Cinque, D. Parisi, A. Roda, F. D. Piaz, M. H. Moon and B. R. Min, *Anal. Chem.*, 2005, **77**, 47–56.
22 D. Kang and M. H. Moon, *Anal. Chem.*, 2005, **77**, 4207–4212.
23 D. Kang and M. H. Moon, *Anal. Chem.*, 2006, **78**, 5789–5798.
24 M. H. Moon, P. S. Williams and H. Kwon, *Anal. Chem.*, 1999, **71**, 2657–2666.
25 A. Gross, X.-M. Yin, K. Wang, M. C. Wei, J. Jockel, C. Milliman, H. Erdjment-Bromage, P. Tempest and S. J. Korsmeyer, *J. Biol. Chem.*, 1999, **274**, 1156–1163.
26 M. H. Moon, D. Kang, I. Hwang and P. S. Williams, *J. Chromatogr., A*, 2002, **955**, 263–272.
27 D. Kang and M. H. Moon, *Anal. Chem.*, 2004, **76**, 3851–3855.
28 M. Reers, T. W. Smith and L. B. Chen, *Biochemistry*, 1991, **30**, 4480–4486.
29 E. Mortz, T. N. Krogh, H. Vorum and A. Gorg, *Proteomics*, 2001, **1**, 1359–1363.
30 M. H. Moon, S. Myung, M. Plasencia, A. Hildebrand and D. E. Clemmer, *J. Proteome Res.*, 2003, **2**, 589–597.
31 D. Kang, H. Nam, Y.-S. Kim and M. H. Moon, *J. Chromatogr., A*, 2005, **1070**, 193–200.
32 R. Beckett and J. C. Giddings, *J. Colloid Interface Sci.*, 1997, **186**, 53–59.
33 P. V. Bondarenko, D. Chelius and T. A. Shaler, *Anal. Chem.*, 2002, **74**, 4741–9.
34 D. Chelius, T. Zhang, G. Wang and R.-F. Shen, *Anal. Chem.*, 2003, **75**, 6658–6665.
35 K. Iwasa, M. Moriyasu, T. Yamori, T. Turuno, D.-U. Lee and W. Wiegrebe, *J. Nat. Prod.*, 2001, **64**, 896–898.
36 H. Fu, W. Li, Y. Liu, Y. Lao, W. Liu, C. Chen, H. Yu, N. T. K. Lee, D. C. Chang, P. Li, Y. Pang, K. W. K. Tsim, M. Li and Y. Han, *J. Proteome Res.*, 2007, **6**, 2435–2446.
37 R. Cao, Z. L. Liu, X. Peng, W. Hu, X. Wang, P. Chen, J. Xie and S. Liang, *J. Proteome Res.*, 2006, **5**, 634–642.
38 J. Tang, C. Faustman, R. A. Mancini, M. Seyfert and M. C. Hunt, *J. Agric. Food Chem.*, 2005, **53**, 5449–5455.
39 P. L. Piotrowski, B. G. Sumpter, H. V. Malling, J. S. Wassom, P. Y. Lu, R. A. Brothers, G. A. Sega, S. A. Martin and M. Parang, *J. Chem. Inf. Model.*, 2007, **47**, 676–685.
40 H. G. Shertzer, G. L. Bannenberg, H. Zhu, R.-M. Liu and P. Moldeus, *Chem. Res. Toxicol.*, 1994, **7**, 358–366.